Effects of UAS-Specific Capacity Constraints on Delays and Aircraft Encounters

Chunki Park[*] and Hak-Tae Lee[†]

University of California Santa Cruz, Moffett Field, CA 94035, USA

This paper presents the impacts of Unmanned Aircraft System (UAS)-specific sector capacity constraints on the delay of UAS and the number of encounters between UAS and manned aircraft. The capacity constraints – represented by a limit placed on the number of aircraft allowed in a given sector – are satisfied by delaying the departure times of UAS that would otherwise exceed the constraint while preserving the intended routes of flights. A first-come first-served departure scheduler is used to determine departure times delays for UAS that satisfy the UAS-specific sector capacity constraints. In this paper, using both time-based and distance-based criteria for determining the aircraft encounters, the conflict risk for different UAS-specific capacity constraints is analyzed. Fast-time simulation results show that the number of encounters generally decreases as the UAS-specific sector capacity is reduced. When the capacity constraints are two times tighter, the number of encounters is reduced by up to 42%. The results also show a general trend toward increased departure delay for UAS as the capacity constraints get tighter.

I.   Introduction

The demand for Unmanned Aircraft Systems (UAS) operations is expected to rapidly grow,[1,2] and thus the safe integration of UAS into the National Airspace System (NAS) has been a collective goal of many organizations such as the Federal Aviation Administration (FAA), Joint Planning and Development Office (JPDO), and National Aeronautics and Space Administration (NASA). Several concepts of operations have been proposed to integrate UAS into the NAS;[3,4] however, the impact of UAS operations on the NAS has not been widely investigated.

Recently, Mueller et al.[5] investigated the effects of typical UAS missions and performance characteristics on existing NAS traffic. They analyzed the impact of the UAS operations for different independent variables including speed, altitude, and separation criteria for the UAS flights. While their paper quantified the sensitivity to operational parameters, it did not evaluate the impact of pre-departure planning subject to capacity constraints.

One possible task in pre-departure planning is to generate the UAS flight plans that avoid the congested airspace to reduce the conflict risks to manned flights. In order to introduce UAS into today's airspace, there may be consideration of setting a different capacity constraint for allowing a UAS to enter a sector. This is referred to as a UAS-specific capacity constraint. In this study, the effects of UAS-specific sector capacity constraints are examined. To satisfy the UAS-specific capacity constraints, a pre-departure planning process in terms of UAS departure scheduling is considered. The UAS departure scheduler adjusts the departure times of UAS to avoid congested airspaces, which will lower the conflict risks, under the assumption that the UAS operations are relatively time-insensitive. The main goal of the study is to examine the change in the encounters between UAS and manned aircraft when the UAS operations are restricted more tightly than manned aircraft operations. This paper presents how the number of encounters and average UAS departure delay vary for different capacity constraints applied to the sectors in which the UAS operate.

This paper is organized as follows: Section II presents the baseline departure scheduler and the modified scheduler for UAS departure scheduling; Section III describes experimental studies that show the effects of

---

[*]Senior Systems/Simulation Engineer, U.C. Santa Cruz, M/S 210-8, Member AIAA, chunki.park@nasa.gov
[†]Scientist, U.C. Santa Cruz, M/S 210-8, Member AIAA, haktae.lee@nasa.gov
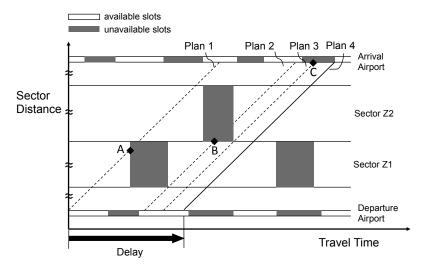
American Institute of Aeronautics and Astronautics

Figure 1: A delay solution using the baseline FCFS departure scheduler.

UAS departure scheduling on the NAS; and Section IV provides conclusions and discusses the directions for future research.

II.   UAS Departure Scheduling

As the air traffic activity is a function of time, the conflict/collision risk for a UAS varies with departure time. Therefore, scheduling departure times for UAS flights may increase or reduce potential risks for conflicts between manned aircraft and unmanned aircraft. A fast time simulation was used to study the effect of UAS-Specific Capacity Constraints on potential conflicts. In this section, an existing baseline first-come first-served (FCFS) departure scheduler is reviewed, and then the modifications of the baseline scheduler for the study are presented.

A.   A First-Come First-Served Departure Scheduler

The baseline FCFS departure scheduler[6,7] creates a departure schedule on a FCFS basis. The scheduler takes several inputs. One of the inputs is a list of flight plans for all fights. A flight plan includes departure airport, departure time, destination airport, arrival time, and entry/transit/exit times for each sector through which the flight flies. Another input is a set of airport departure and arrival capacities. It also requires sector capacity limits.

The scheduler sorts all flights according to the original flight-plan departure time, and then starts scheduling by allocating the airport and sector resources to the flights. When a flight departs from an airport, a pre-specified time period around the departure time is set to an occupied interval for the airport to maintain safe separation from other flights. The scheduler derives the amount of time period from the departure capacity of each airport. The same algorithm is applied to the arrival time. Once a flight is scheduled, the available capacity of each sector the flight flies through is reduced by one during the transit time. If its available capacity reaches zero for a time period, other subsequent flights are not permitted to fly into this sector during the period, and so delays are expected for them. To find the next available time intervals, the scheduler needs to shift all times forward, including departure time, arrival time, and entry/exit times for all sectors it passes through, in the original flight plan. This time shift represents a departure delay for the flight.

Figure 1 shows how the scheduling algorithm works. Each row corresponds to a unique NAS resource: an airspace sector or an airport. The grey regions in sector rows indicate the time intervals in which the maximum capacities of the sectors are reached, and those in airport rows represent the time periods that have already been occupied by the formerly scheduled flights. The one slanted solid line represents a feasible delay solution, and the three dashed lines are unfeasible plans. All four lines have the same slope since their transit times are not altered from the nominal transit times. Plan 1 does not have any constraint violations

American Institute of Aeronautics and Astronautics

in Sector Z2; however, it violates the constraint on Sector Z1 (Point A). Plan 2 is unfeasible since it tries to enter Sector Z2 during the period in which the maximum capacity has been reached (Point B). Plan 3 satisfies all sector constraints but its arrival time is within the blocked period at the arrival airport (Point C). Therefore, Plan 4 is the feasible solution that satisfies all sector and airport constraints with a minimum departure delay. The scheduler updates airport and sector resource availabilities with respect to time, and then repeats this procedure until it schedules the last flight.

B.   A Modified Scheduler for UAS Departure Scheduling

As mentioned earlier, the objective of this study is to investigate the effect of UAS-specific capacity constraints on UAS flight delays and aircraft encounters. To this end, the baseline scheduler was modified to alter only the departure times of UAS to satisfy the capacity constraints at the sectors that they fly through. For convenience, the modified version of scheduler will be called *UAS Departure Scheduler*. As a first step, this paper assumes that it is permissible for a UAS flight to enter a sector only when the sector's total aircraft count, which includes both manned and unmanned aircraft, does not exceed a pre-specified number during its transit time. In this paper, this number is defined as the UAS Monitor Alert Parameter (UMAP).

The mission types being planned for UAS of the future are rarely point-to-point, which is a typical type of manned aircraft, but generally involve several forms of patterned flights such as circular or racetrack loitering patterns.[2] These different patterns of UAS flights may result in more complex air traffic than manned aircraft. Therefore, in this paper, the UAS-specific sector capacity constraint, that is UMAP, is proposed, and the effect of imposing UMAP on UAS flights on the NAS is investigated. Currently, the workload impact of an unmanned aircraft is not clearly known compared to a manned aircraft. So, the UMAP introduced in this study may not have a one-to-one relationship with the conventional Monitor Alert Parameter.

Since sector constraint violations by manned aircraft are not the main focus of this study, only the UAS flights are rescheduled. To minimize the disruption of the manned traffic, the UAS departure scheduler first populates the sector resource status using the original schedule of all the manned flights. Then, for a given UMAP value, it determines the appropriate departure time delay for each UAS flight in conformance with all sector constraints.

Figure 2 describes an example of scheduling the UAS flight's sector entry time for a given UMAP value of 17. After simulating all manned aircraft, the UAS departure scheduler obtains traffic history data for each sector as a function of time. Step (a) shows the resulting traffic data for one of the sectors that the UAS plans to fly through. The UAS flight is not allowed to enter this sector at its original scheduled entry time since the sector capacity has already reached the specified UMAP value of 17 during a part of its original transit period as shown in step (b). Therefore, the scheduler looks for the next available time period that satisfies the constraint on the given UMAP value. Step (c) shows a feasible sector transit period as determined by the scheduler. This figure shows an example for a single sector case; however, the scheduler carries out this scheduling process simultaneously for all sectors that the UAS plans to fly through and finally determines the departure time delay as much as needed.

III.   Experiments

It is hypothesized here that the number of encounters involving UAS will increase as higher UMAP values are given to the scheduler. In this paper, an encounter is defined as a pair of aircraft that at a certain point have their relative state below a given threshold; the relative state between two aircraft is defined by either separation distance or simple τ. The simple τ means the time to closest point of approach, and it is calculated by dividing range by closure rate.[8] In this study, the number of encounters is considered as the potential conflict risk. Therefore, this hypothesis also means that UAS flights will have greater risk of conflict with manned aircraft when they are allowed to enter busier sectors. Another hypothesis is that as the UMAP value decreases, the number of encounters will decrease but the UAS departure delay will increase. This section describes the experimental setup for testing those hypotheses and reports the results that show the effects of UAS-specific capacity constraints.

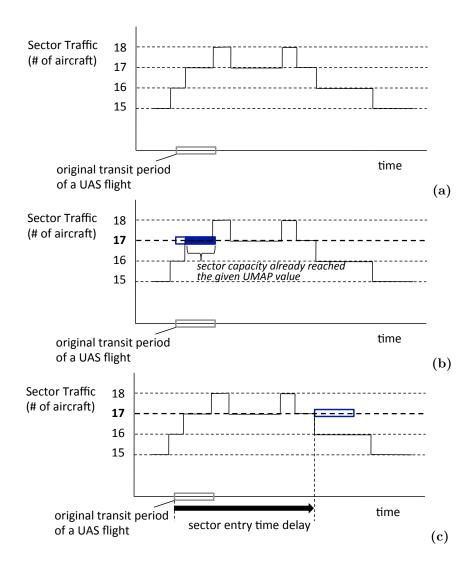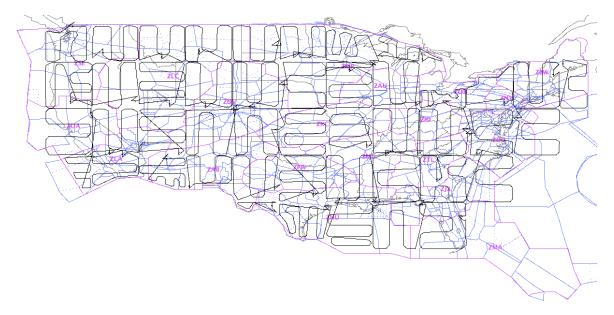American Institute of Aeronautics and Astronautics

Figure 2: The revised sector entry time that the UAS depature scheduler determines according to a given UMAP value of 17. (a) After simulating all manned aircraft, the UAS departure scheduler obtains traffic history data for sectors as a function of time. This plot depicts traffic demand for one of the sectors that the UAS plans to pass through. (b) The UAS' original scheduled transit period for this sector is not allowable since the sector capacity has already reached the given UMAP value during a part of the period. (c) So, the scheduler searches the next available time that satisfies the constraint on the specified UMAP value.

A. Experimental Setups

Using the flight plans for background traffic and the UAS flight plans that are modified by the UAS departure scheduler, a fast-time NAS-wide simulation tool carries out the simulation runs. Airspace Concept Evaluation System (ACES) Build 6.6 is used as the simulation tool. ACES can run a gate-to-gate simulation of air traffic at local, regional and national levels.[9] It simulates flight trajectories using aircraft models derived from the Base of Aircraft Data (BADA)[10] and traffic data consisting of departure times and flight plans obtained from recorded Airline Situation Display to Industry (ASDI) files.

Two scenarios in Fig. 3 are used for the ACES simulations. One performs atmospheric sampling missions over all 20 Air Route Traffic Control Centers (ARTCCs) in the NAS using 48 UAS flights. The cruise altitude of each UAS flight is FL360 and the cruise speed is 340 knots. The other scenario performs aerial photography missions using 12 UAS fights in congested airspace only. The cruise altitude and speed of each UAS flight is FL340 and 200 knots, respectively. Both scenarios contain background traffic of manned

American Institute of Aeronautics and Astronautics

(a) NAS-wide UAS Atmospheric sampling mission profile.

(b) Aerial photography mission profile in congested airspace only. The flight pattern of each UAS is shown in the box on the bottom left.

Figure 3: UAS traffic scenarios, UAS tracks in black.

aircraft for a 24-hour period on Wednesday, July 25, 2012, which includes approximately 50,000 manned flights.

As shown in Fig. 4, using each scenario, ACES runs the baseline simulation to generate a list of unimpeded flight plans for all flights. Then, using the flight plans, the UAS departure scheduler determines feasible departure time for each UAS flight while it varies the UMAP values from 9 to 18 with no change in the departure times for manned aircraft.

After the UAS departure times in the baseline flight plans are adjusted according to the result from
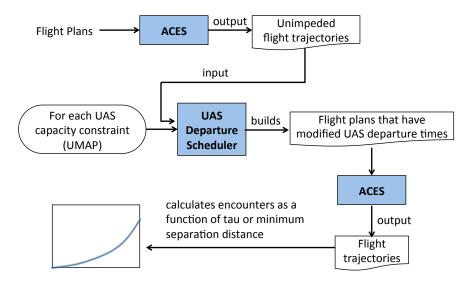
American Institute of Aeronautics and Astronautics

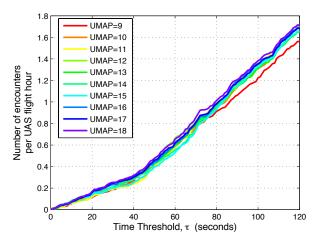Figure 4: Overall experiment procedure

the UAS departure scheduler, ACES simulation is performed again with the adjusted schedule. Next, the recorded aircraft trajectories are analyzed, and then the number of encounters are calculated as both a function of simple range τ and a function of minimum separation distance. To consider the en-route portion of the UAS flights, only the pairs of the UAS flight and manned aircraft at 11,000 ft or above are analyzed. This process is repeated until the UAS departure schedules for all given UMAP values are simulated and analyzed. In these ACES simulations, no separation assurance function is modeled.
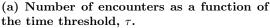
In summary, an independent variable for experiments is the UMAP value that varies from 9 to 18. The other independent variable is the UAS mission scenario. This paper investigates two UAS mission scenarios: one covers entire U.S., and the other is operating only in congested airspace. The dependent variables are the number of encounters per UAS flight hour and the average per UAS departure delay.
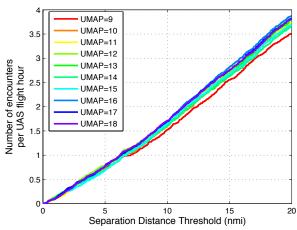
B.   Results from Atmospheric Sampling Missions

The results from the ACES simulations for atmospheric sampling missions that covered the entire contiguous United States are presented in this subsection. Figure 5a shows that the number of encounters per UAS flight hour increased as the τ increased. This figure also shows an increasing trend in the number of encounters for large time thresholds with higher UMAP values. However, it was difficult to observe similar tendencies for τ less than around 80 seconds. Similar to these time threshold results, the separation distance threshold results show that the number of encounters per UAS flight hour increased as the distance threshold increased as depicted in Fig. 5b. Figure 5c shows the number of aircraft encounters per UAS flight hour as a function of the UMAP values. There was little difference in the number of encounters for different UMAP values; however, as the threshold was increased, the difference became more pronounced.
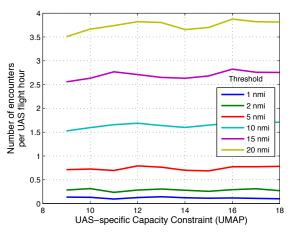
As the UMAP value was decreased, the UAS departure delay increased as expected. When the UMAP value was set to 18, the average delay for UAS was 3.5 minutes. As shown in Fig. 5d, the average delay was slightly increasing until the UMAP value decreased to 14; however, the delay was increasing steeply when the UMAP was less than 13. It was 3.16 hours when the MAP value was 9. Figure 5d also shows the relationship between the number of encounters per UAS flight hour and the UAS departure delays as a function of the UMAP value when the separation distance threshold was set to 5 nmi, which is the legal horizontal separation distance for air traffic control. Using this trade-off graph, the UAS departure times might be determined to reduce conflict risk. For example, if the objective was to find the UAS departure delay with the minimum conflict risk, the delay would be chosen at the UMAP value of 15, which was 6.5 minutes. Although this presents the straightforward trade-off study, further investigations that include robustness and uncertainties should also be conducted.
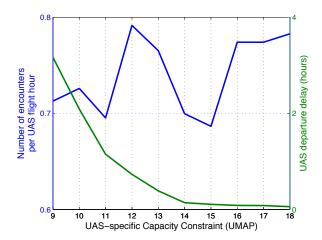
American Institute of Aeronautics and Astronautics

(a) **Number of encounters as a function of the time threshold, τ.**

(b) **Number of encounters as a function of separation distance threshold.**

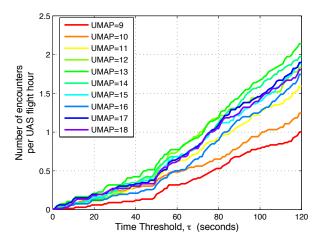(c) **The number of encounters per UAS flight hour as a function of the UMAP value.**
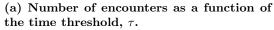

(d) **The relationship between the number of encounters per UAS flight hour and the UAS departure delays (when the separation distance threshold is set to 5 nmi).**
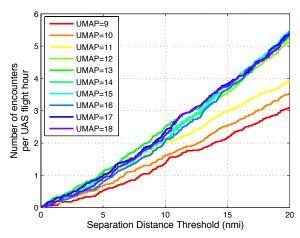
Figure 5: Results for the scenario of atmospheric sampling missions that cover the entire contiguous United States
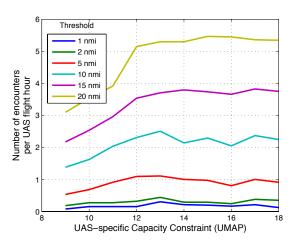
C. Results from Aerial Photography Missions

This subsection presents the results from the ACES simulations for aerial photography missions that operated in congested airspace. As in the results for atmospheric sampling missions, the number of encounters per UAS flight hour increased as τ increased as shown in Fig. 6a. The number of encounters in Fig. 6b was also higher when the separation distance threshold was increased more. Compared to the atmospheric sampling mission results, both figures more distinctly show a general trend of more encounters when a higher UMAP value was given; however, it was still difficult to observe this trend at the lower thresholds. Figure 6c depicts the number of encounters as a function of the UMAP and shows this trend clearly. Another observation was that the number of encounters for higher UMAP values was often smaller than that for lower UMAP values even when large thresholds were given. This might happen since other factors such as UAS departure times and characteristics of background traffic could also make a big impact on the number of encounters. Further investigation should be done in the future work.
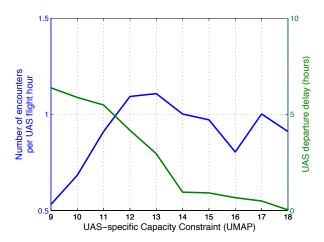
American Institute of Aeronautics and Astronautics

(a) Number of encounters as a function of the time threshold, τ.

(b) Number of encounters as a function of separation distance threshold.

(c) The number of encounters per UAS flight hour as a function of the UMAP value.

(d) The relationship between the number of encounters per UAS flight hour and the UAS departure delays (when the separation distance threshold is set to 5 nmi).

Figure 6: Results for the scenario of aerial photography missions in congested airspace only

As shown in Fig. 6d, when the UMAP value was decreased, the UAS departure delay was higher as in the results for atmospheric sampling missions. When the UMAP value was 18, the average delay for UAS flights was less than 2 minutes. Similar to the prior results, the average delay was gradually increasing until the UMAP value was decreased to 14, but the delay increased rapidly at the UMAP values lower than 13. The average delay was 6.38 hours at the UMAP value of 9. Figure 6d also presents the relationship between the number of encounters per UAS flight hour and the UAS departure delays as a function of the UMAP value when the separation distance threshold was set to 5 nmi. Similar to atmospheric sampling mission results, this trade-off figure could be used to determine the proper departure times for UAS flights.

IV.   Concluding Remarks

This paper analyzed the effect of UAS-specific capacity constraints on aircraft encounters and UAS flight delays. Capacity constraints are enforced using a pre-departure UAS scheduler. To examine the effects,

American Institute of Aeronautics and Astronautics

a fast-time simulation tool, ACES, was used. Using two traffic scenarios, one of which covers the entire NAS and the other only congested airspace, it ran experimental simulations. The results corroborate the hypothesis that higher UMAP values yield more encounters. This means that the UAS flight has higher risk of conflict with manned flights when it is allowed to enter busier sectors. The trend is much more pronounced in congested airspace. In the result from the congested airspace mission, the number of encounters per UAS flight hour was reduced by up to 42% when the UMAP value decreased from 18 to 9. However, it is difficult to observe this trend for small threshold values. The experimental results also suggest that lower UMAP values produce longer UAS departure delays.

Although this study showed the general trend that the number of encounters per UAS flight hour decreases as the UAS-specific capacity decreases, it was sometimes difficult to observe this trend with the higher UMAP value even for the large threshold. Therefore, future research should investigate what other factors impact the conflict risk.

Acknowledgments

References

[1]Lacher, A., Zeitlin, A., Maroney, D., Markin, K., Ludwig, D., and Boyd, J., "Airspace Integration Alternatives for Unmanned Aircraft," Tech. rep., The MITRE Corporation, Feb. 2010.

[2]DeGarmo, M. and Nelson, G., "Prospective Unmanned Aerial Vehicle Operations in the Future National Airspace System," *Proceedings of the 4th AIAA Aviation Technology, Integration, and Operations (ATIO) Forum*, September 2004.

[3]Federal Aviation Administration (FAA), *Integration of Unmanned Aircraft Systems into the National Airspace System: Concept of Operations V2.0*, September 2012.

[4]DeGarmo, M. and Maroney, D., "NextGen and SESAR: Opportunities for UAS Integration," *Proceedings of the 26th International Congress of the Aeronautical Sciences (ICAS)*, Anchorage, Alaska, September 2008.

[5]Mueller, E., Santiago, C., Cone, A., and Lauderdale, T., "Effects of UAS' Performance Characteristics, Altitude and Mitigation Concepts on Aircraft Encounters and Delays," *Air Traffic Control Quarterly (to be published)*, 2013.

[6]Palopo, K., Chatterji, G. B., and Lee, H.-T., "Interaction of Airspace Partitions and Traffic Flow Management Delay," *Proceedings of the 10th AIAA Aviation Technology, Integration, and Operations (ATIO) Conference*, AIAA, Fort Worth, Texas, September 2010.

[7]Park, C., Lee, H.-T., and Meyn, L. A., "Computing Flight Departure Times Using an Advanced First-Come First-Served Scheduler," *Proceedings of the 12th AIAA Aviation Technology, Integration, and Operations (ATIO) Conference*, AIAA, Indianapolis, Indiana, September 2012.

[8]Federal Aviation Administration (FAA), *Sense and Avoid (SAA) for Unmanned Aircraft Systems (UAS) : Second Caucus Workshop Report*, January 2013.

[9]Meyn, L. A., Windhorst, R., Roth, K., Drei, D. V., Kubat, G., Manikonda, V., Roney, S., Hunter, G., Huang, A., and Couluris, G., "Build 4 of the Airspace Concept Evaluation System," *Proceedings of the AIAA Modeling and Simulation Technologies (MST) Conference and Exhibit*, AIAA, Keystone, Colorado, August 2006.

[10]Nuic, A., Poles, D., and Mouillet, V., "BADA: An advanced aircraft performance model for present and future ATM systems," *International Journal of Adaptive Control and Signal Processing*, Vol. 24, No. 10, 2010, pp. 850–866.